MADCOR

In-situ Corrosion Monitoring of 316 SS Molten Salt Loop by Radioactive Isotope Tracking

Yafei Wang[1], Cody Falconer[2,4], Aeli Olson[3], Brian Kelleher[4], Ivan Mitchell[4], Jonathan Engle[3], Kumar Sridharan[1,2], Adrien Couet[1,2]

[1] Department of Engineering Physics, University of Wisconsin-Madison

[2] Department of Materials Science and Engineering, University of Wisconsin-Madison

[3] Department of Medical Physics and Radiology, University of Wisconsin-Madison

[4] TerraPower, LLC

Wang, Y., Olson, A.P., Falconer, C. *et al.* Radionuclide tracing based in situ corrosion and mass transport monitoring of 316L stainless steel in a molten salt closed loop. ***Nature Communications*** **15**, 3106 (2024). https://doi.org/10.1038/s41467-024-47259-8

Department of Engineering Physics
UNIVERSITY OF WISCONSIN–MADISON

TerraPower

OAK RIDGE National Laboratory

NEUP
Nuclear Energy University Programs

MOTIVATION

- Corrosion is a main concern in molten salt applications.
- Mass transport under flow conditions is rarely studied due to the experimental setup challenges.
- In-situ monitoring of corrosion in molten salt loop would provide valuable data for model validation.

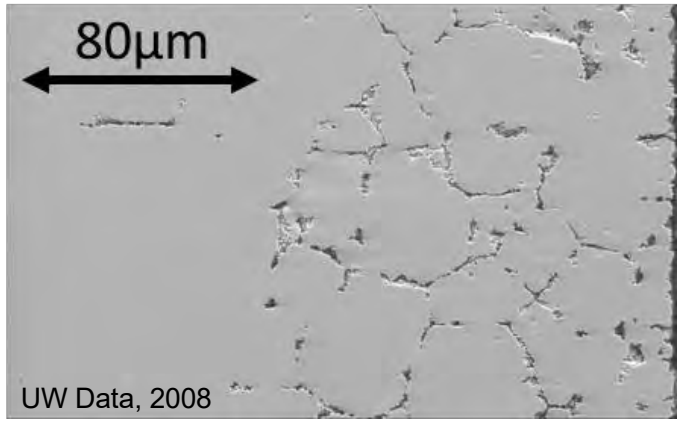

Hastelloy-X (21.3%Cr), 850°C, 500 hours in FLiNaK,

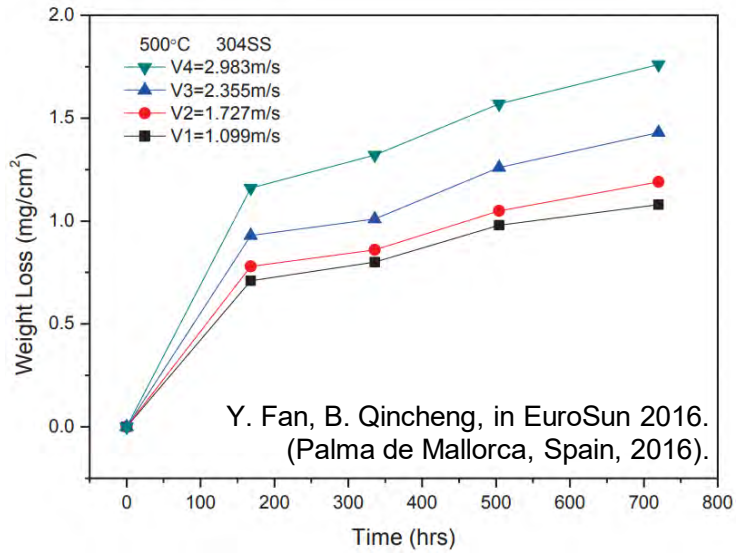

Weight loss for 304 SS after exposure to NaNO3-KNO3 molten salt at 500°C at various fluid velocities

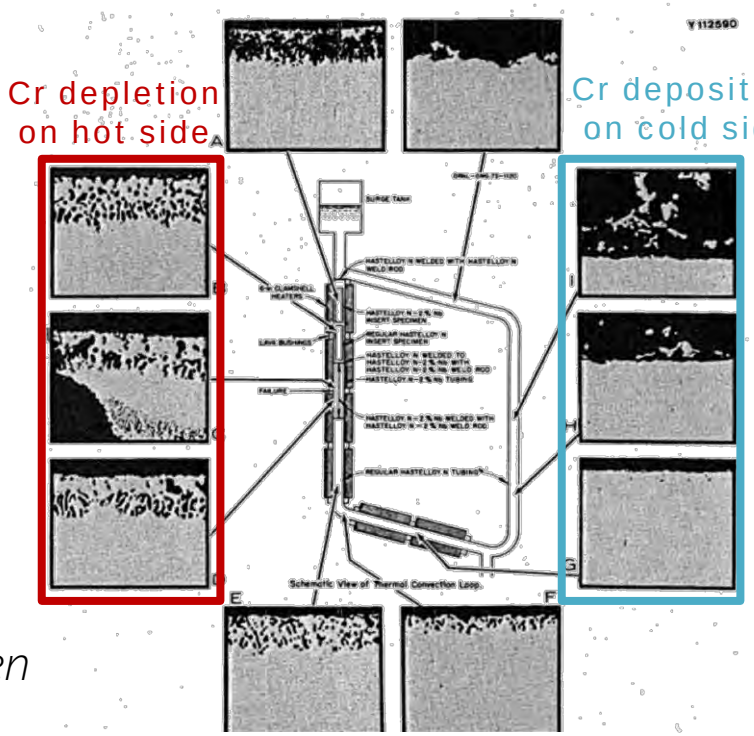

ORNL/MSRE data

Mini Loop Design

Alloy screening in static conditions is good, but ultimately we need data in flowing conditions!

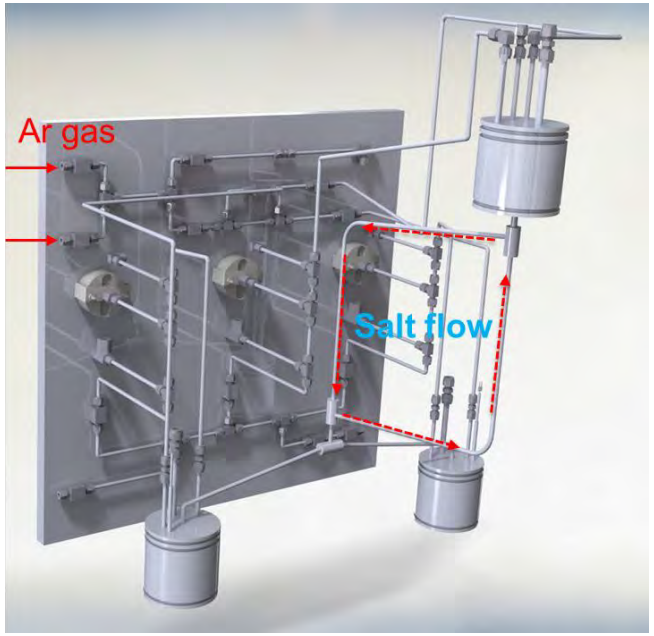

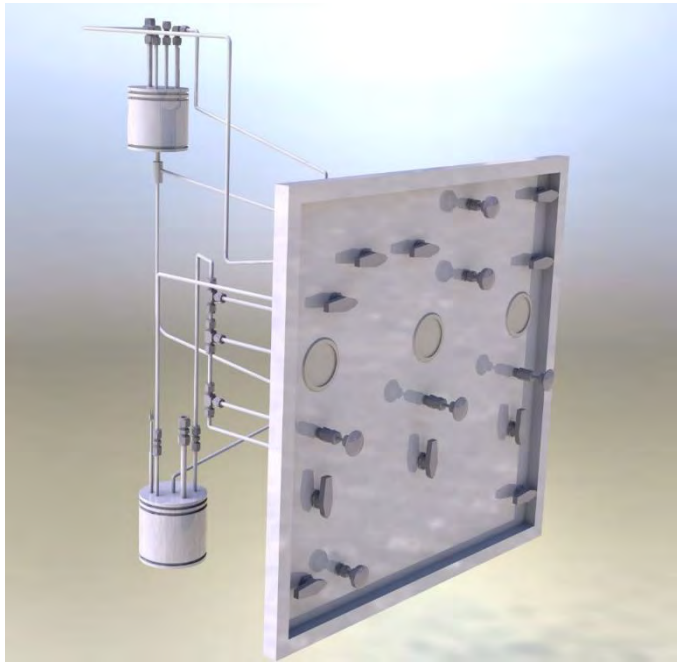

- Dimension: 32″×32″×32″.
- Salt: NaCl-$MgCl_2$ eutectic salt from ORNL.
- Hot leg: 620°C

- Tube: 1/4″, 316 SS L
- Only ~150 g salt needed.
- Cold leg: 500°C

EXPERIMENTAL SETUP OF RADIOISOTOPE TRACKING TECHNIQUE

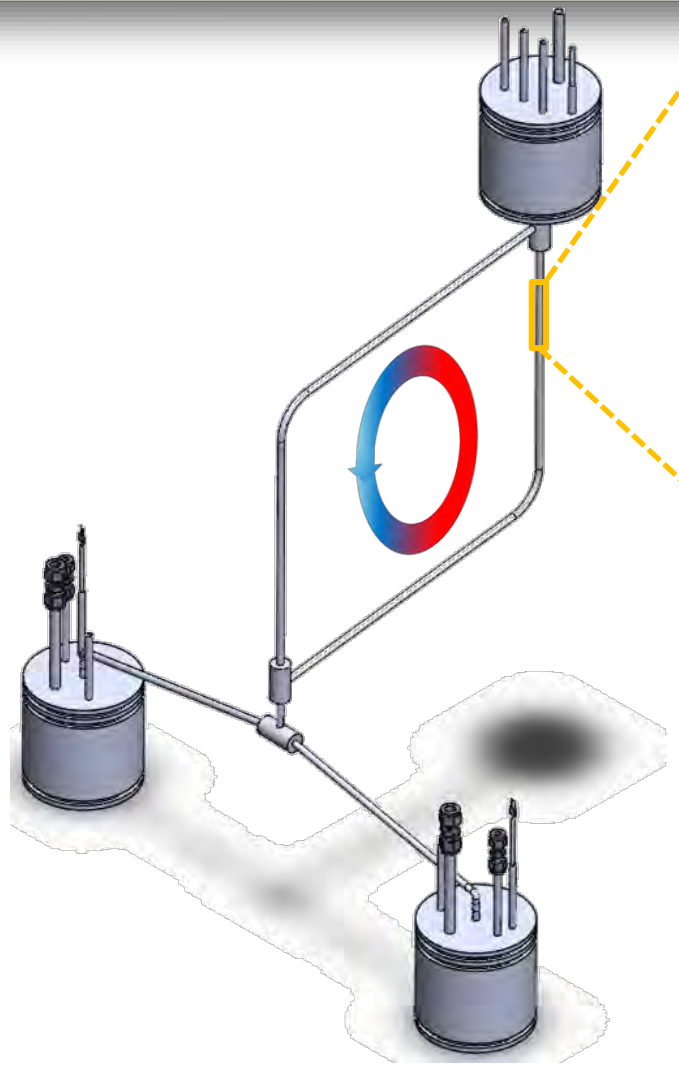

Mini loop schematic

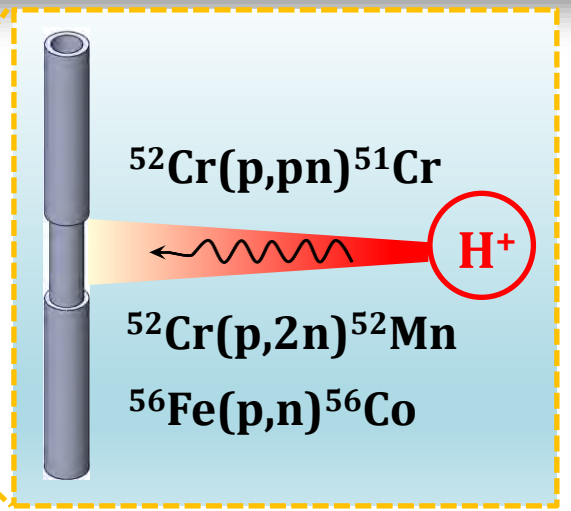

Radioisotope production

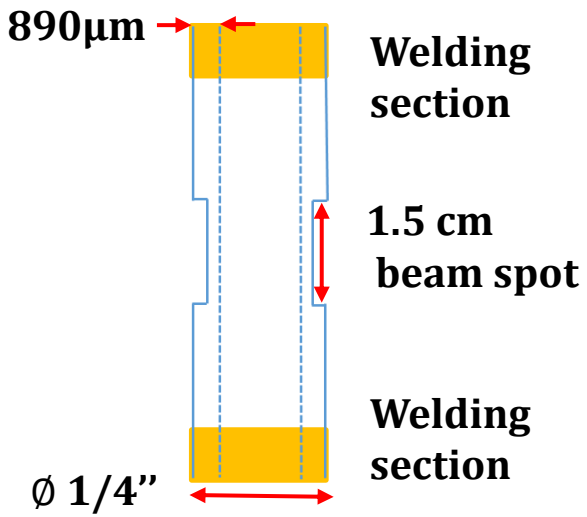

Schematic of irradiated tube section

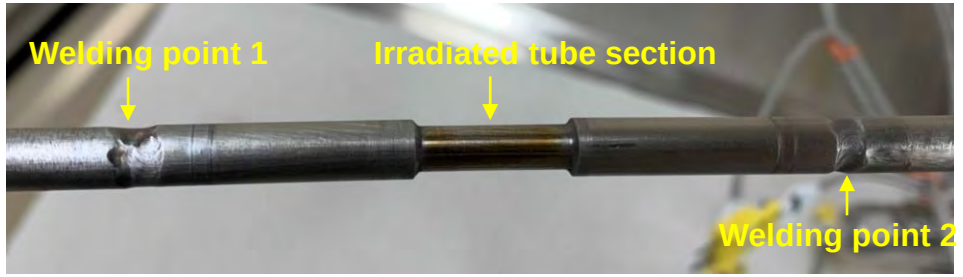

Welded Irradiated tube section

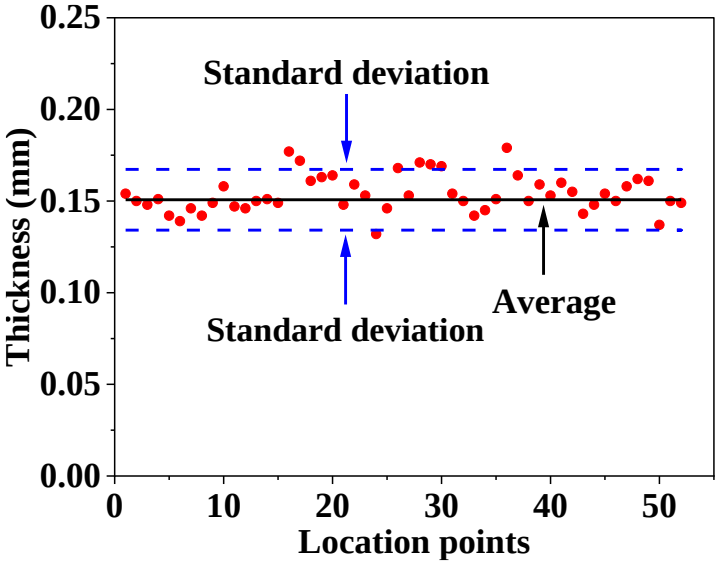

Measurement of irradiated tube thickness

RADIOISOTOPE PRODUCTION AT CYCLOTRON

Cyclotron Activation simulation:

$Cr^{52}(p,pn)\mathbf{Cr^{51}}$, $Cr^{52}(p,n)\mathbf{Mn^{52}}$, $Fe^{56}(p,n)\mathbf{Co^{56}}$

$$A = Nx\sigma I\left(1 - e^{-\lambda t}\right)$$

N= # of target particles per unit area

x= thickness

σ= cross section

I= cyclotron proton bombardment current

λ=decay constant

t= irradiation time

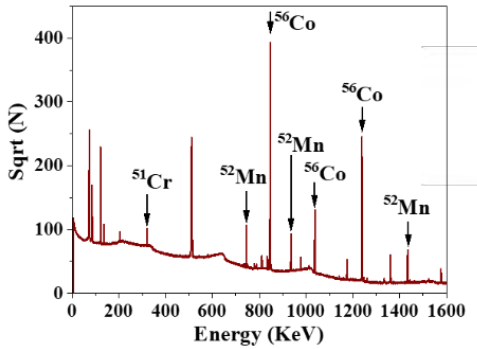

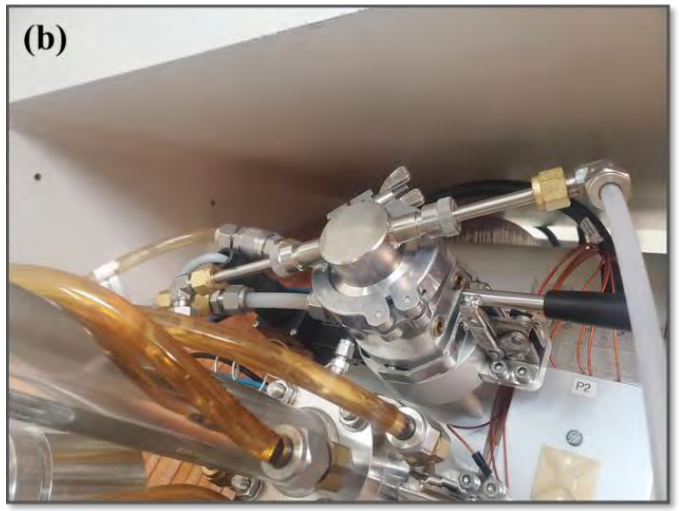

Tube section mounted in chamber before irradiation with 16MeV protons

Modeled activity profile along the 150 µm thick tube

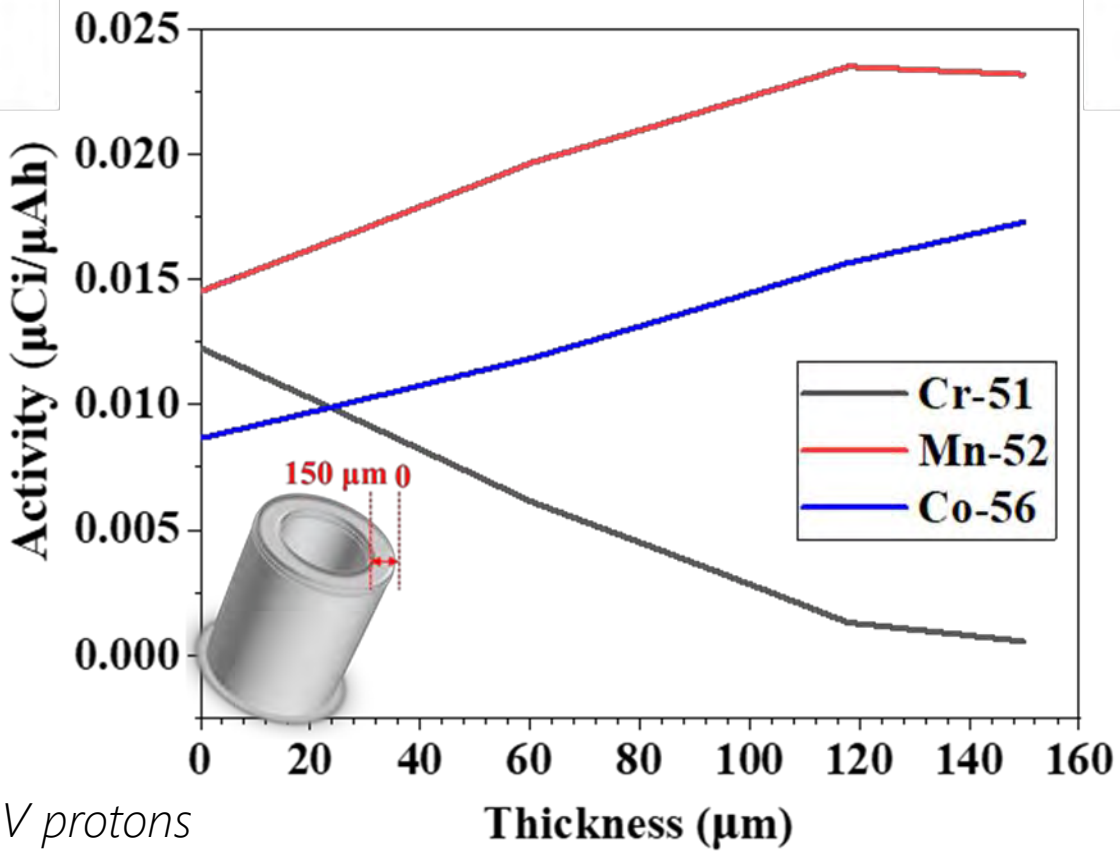

Experimental Validation of Radioisotope Production

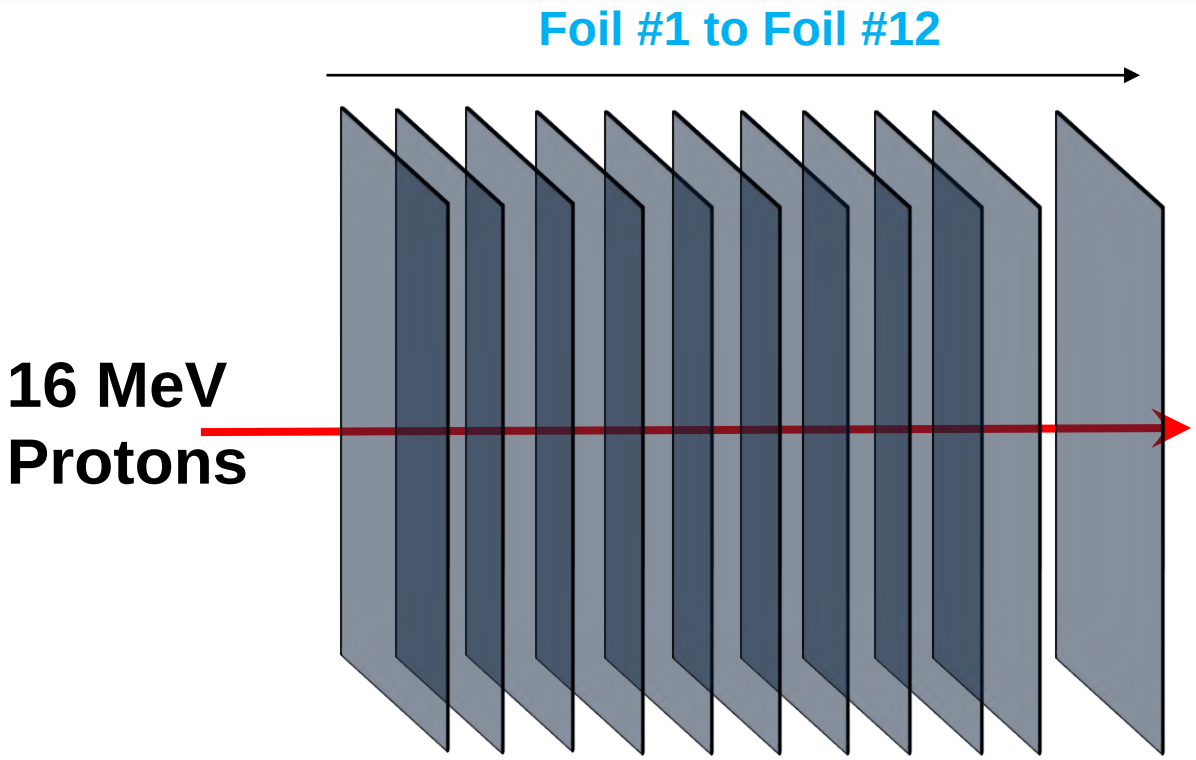

- 316 SS foils with the thickness of 12.5 μm
- Quantity: 12
- Total thickness: 150 μm

Experimental validation of modeled activity as function of tube thickness

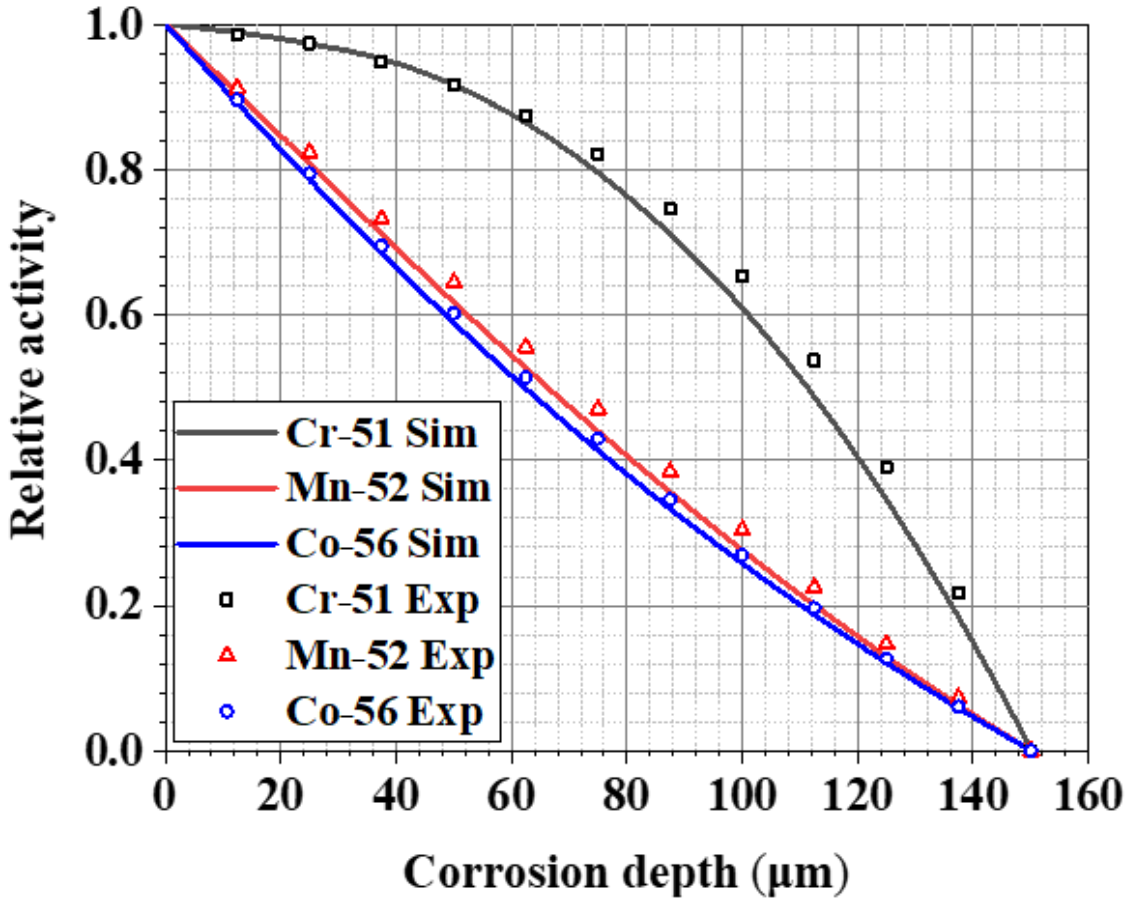

EXPERIMENTAL SETUP OF RADIOISOTOPE TRACKING TECHNIQUE

Micro-loop inside the inert glovebox for salt loading

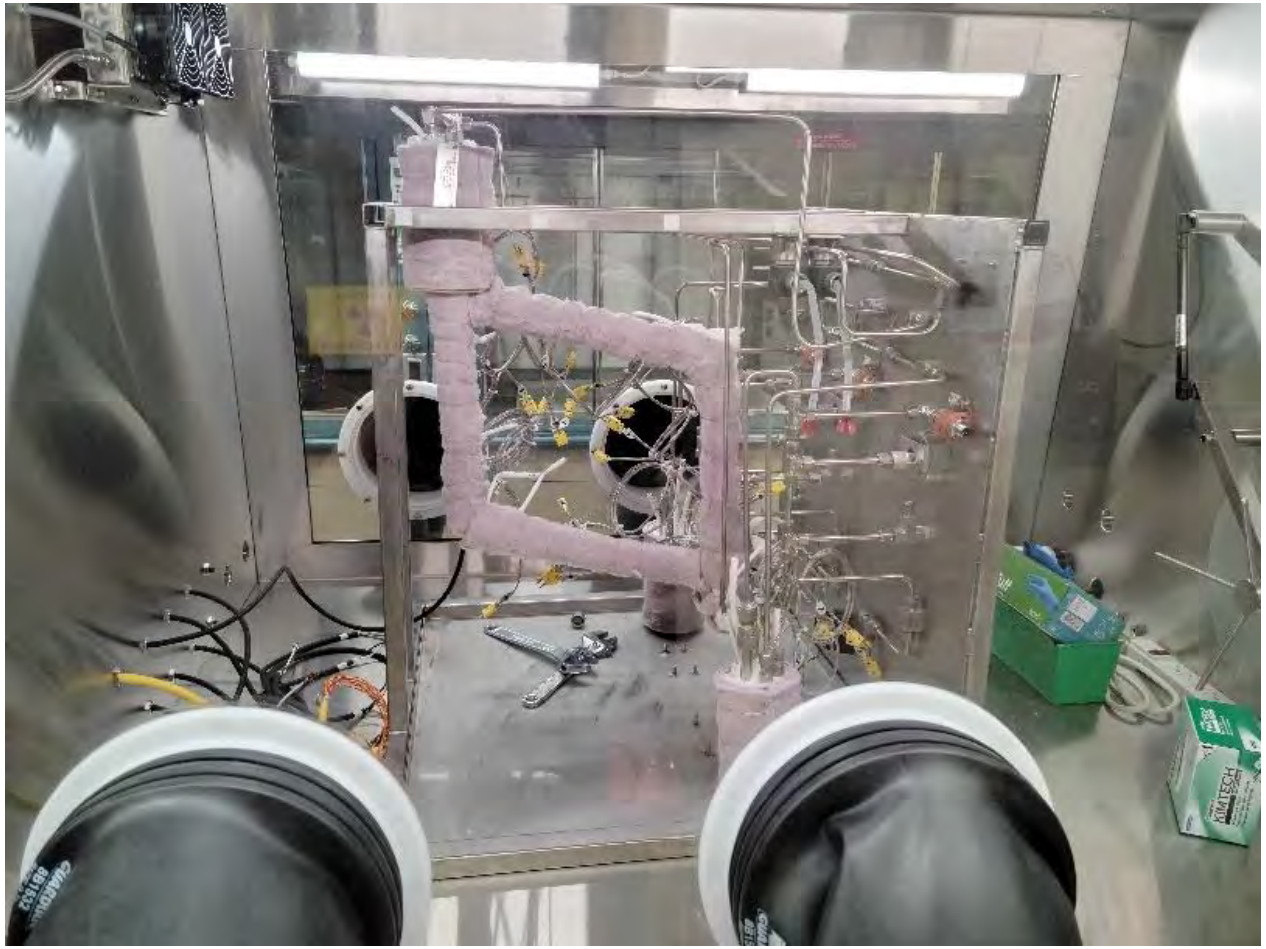

Molten salt : Eutectic NaCl-$MgCl_2$ [58.5-41.5 mol %]

Melting point: 445°C

Total salt: 320 grams (two 96 cm^3)

Temperature of the microloop :
Cold leg temperature = 497.6 ± 4.8°C
Hot leg temperature = 619.9 ± 0.2°C
Temperature gradient = 122.3°C

The main impurities of eutectic NaCl-$MgCl_2$ salt received from Oak Ridge National Laboratory from ICP-MS (in ppm).

#	Li	S	K	Ca	Cr	Mn	Fe	Ni
1	0.51	5.84	27.2	7.47	0.036	0.013	0.141	0.159
2	1.00	5.22	10.6	6.81	0.036	0.014	0.141	0.339
3	0.85	5.27	9.3	6.69	0.025	0.012	0.095	0.177

EXPERIMENTAL SETUP OF RADIOISOTOPE TRACKING TECHNIQUE

Micro loop equipped with 2 HPGe detectors

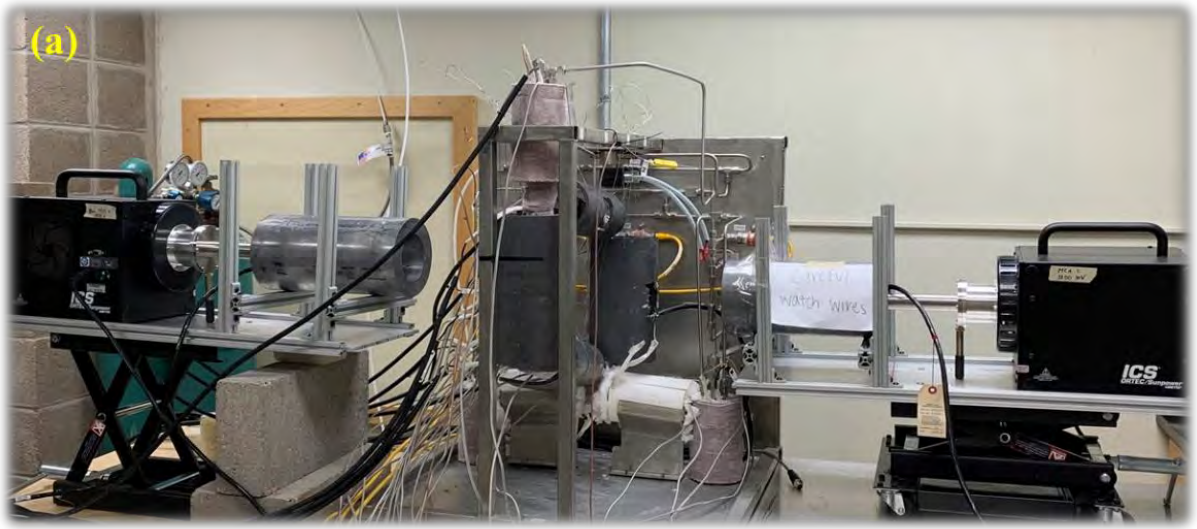

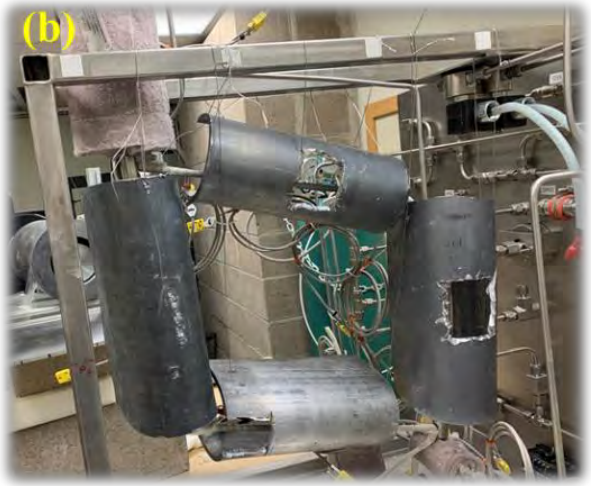

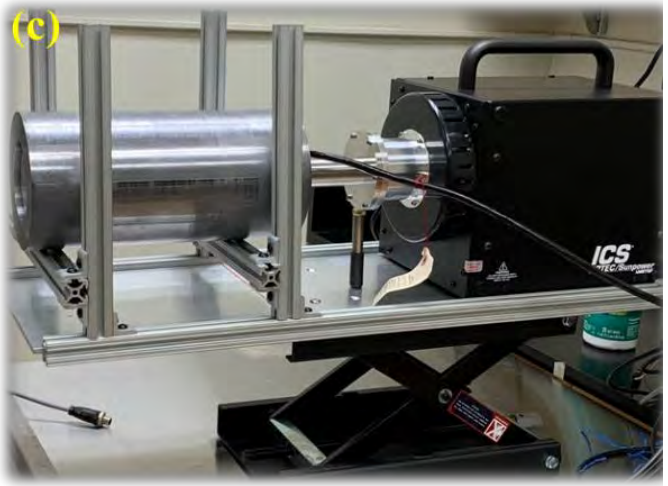

- Detector #2: In situ corrosion monitoring of the tube at hot leg → corrosion rate
- Detector #1: In situ corrosion monitoring on the transportation of corrosion products → mass transport

IN-SITU CORROSION MONITORING AT HOT LEG → CORROSION RATE

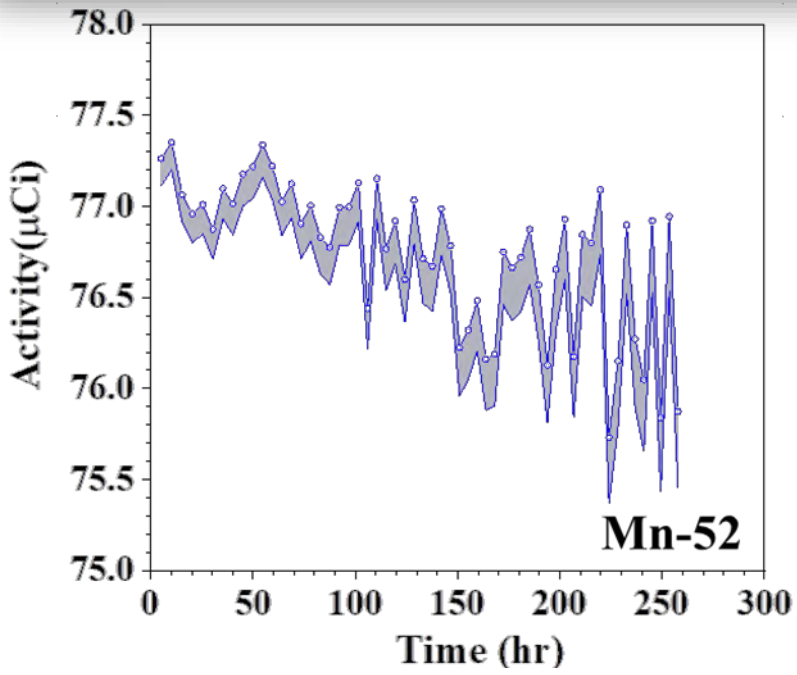

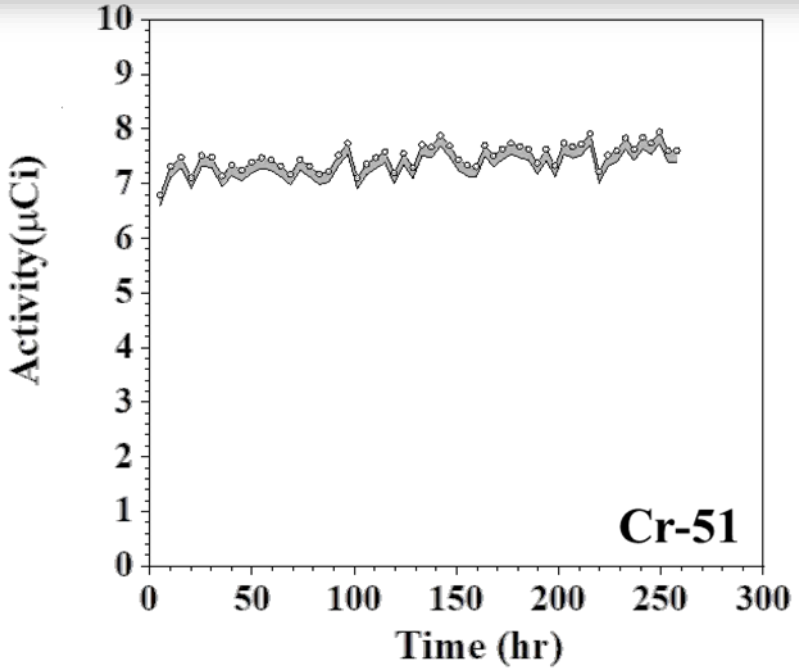

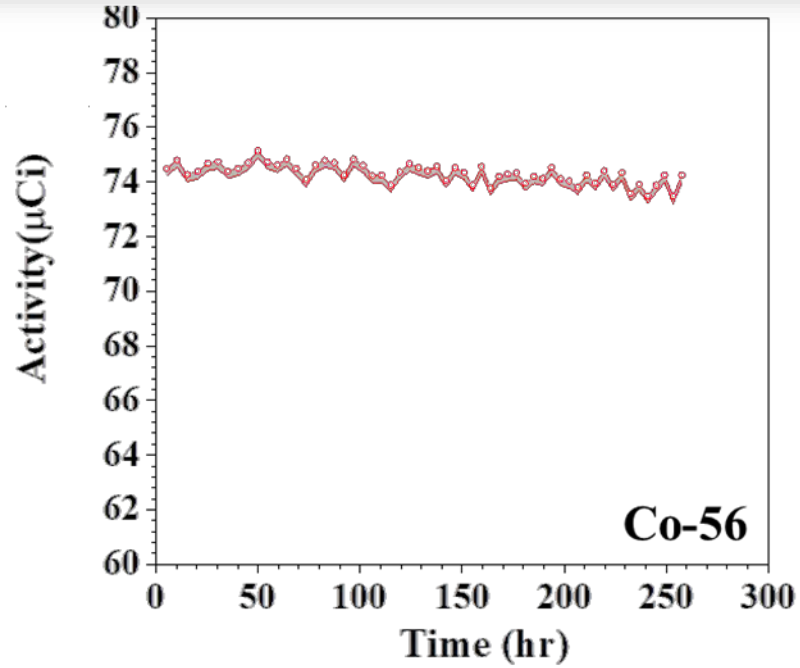

- Loop ran for about 260 hours
- Mn-52: tracer for in-situ monitoring of 316 L loop in a short term.

Irradiated tube failure after about 880 hours

Post Corrosion 316SS Tube Characterizations: Hot Leg

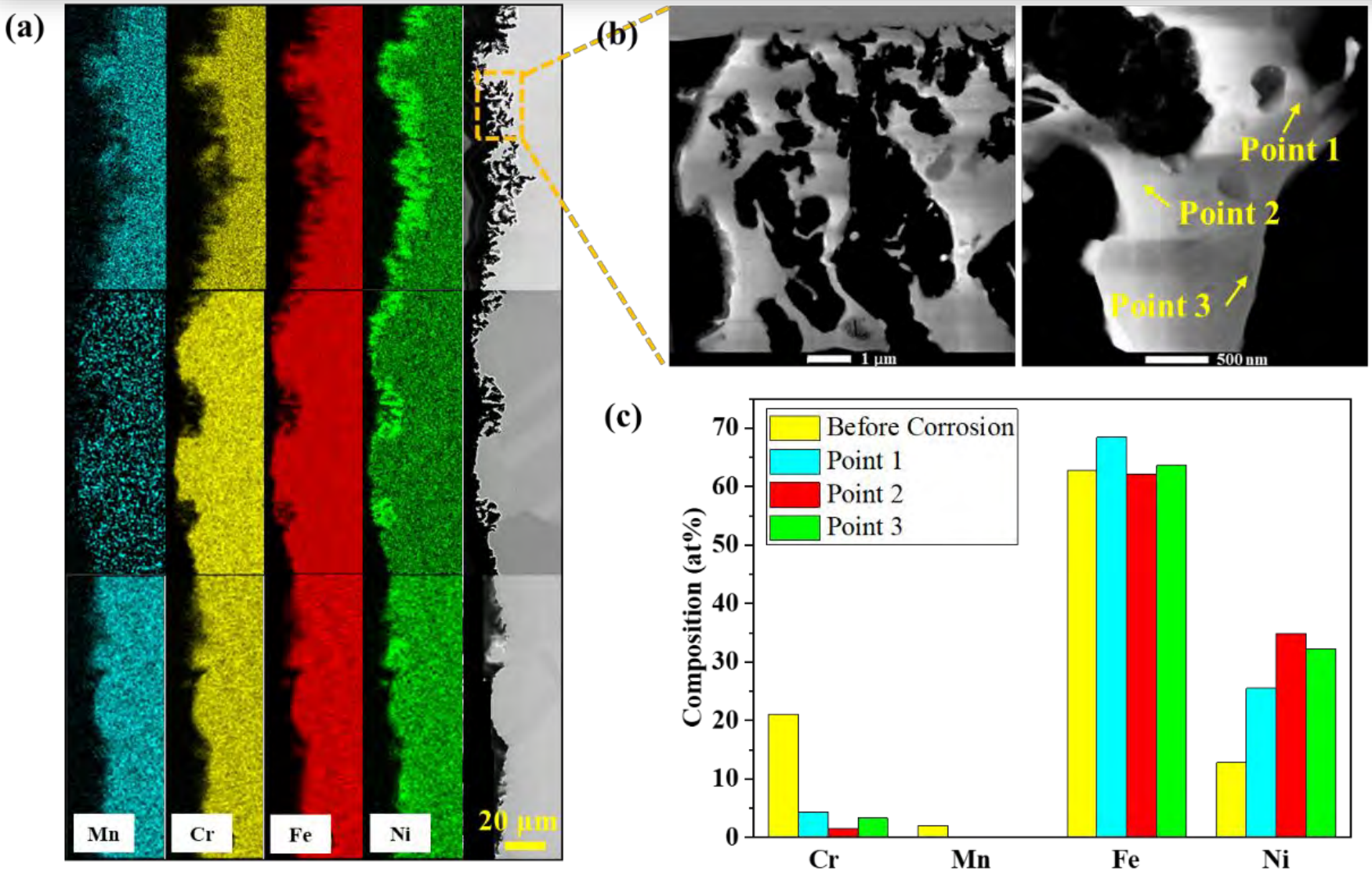

Characterizations of samples after flow loop corrosion testing. (a) SEM image of the tube cross section close to the irradiated section at the hot leg of the loop after loop operation; (b) STEM HAADF images of corroded layer; (c) STEM EDS point scans of the main elements' compositions in the remnants of the 316L SS alloy

POST CORROSION 316SS TUBE CHARACTERIZATIONS COLD LEG

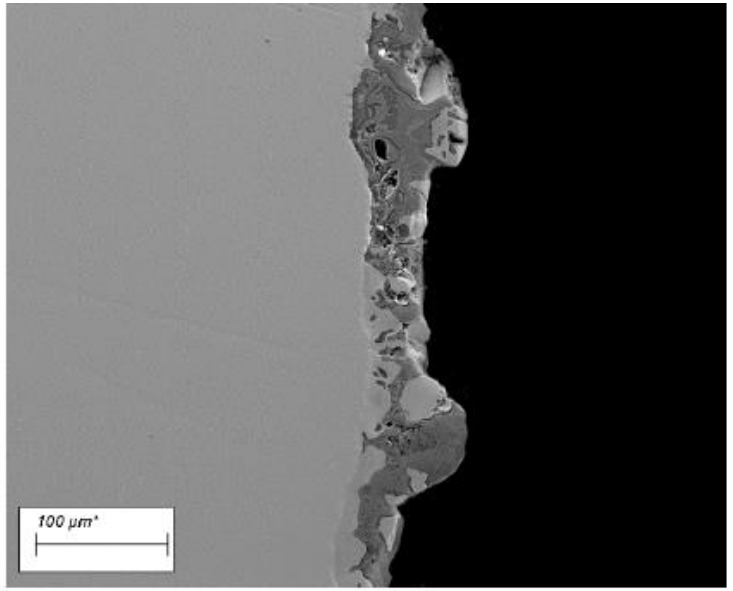

SEM/EDS imaging on the cross section of the tube section from cold leg.

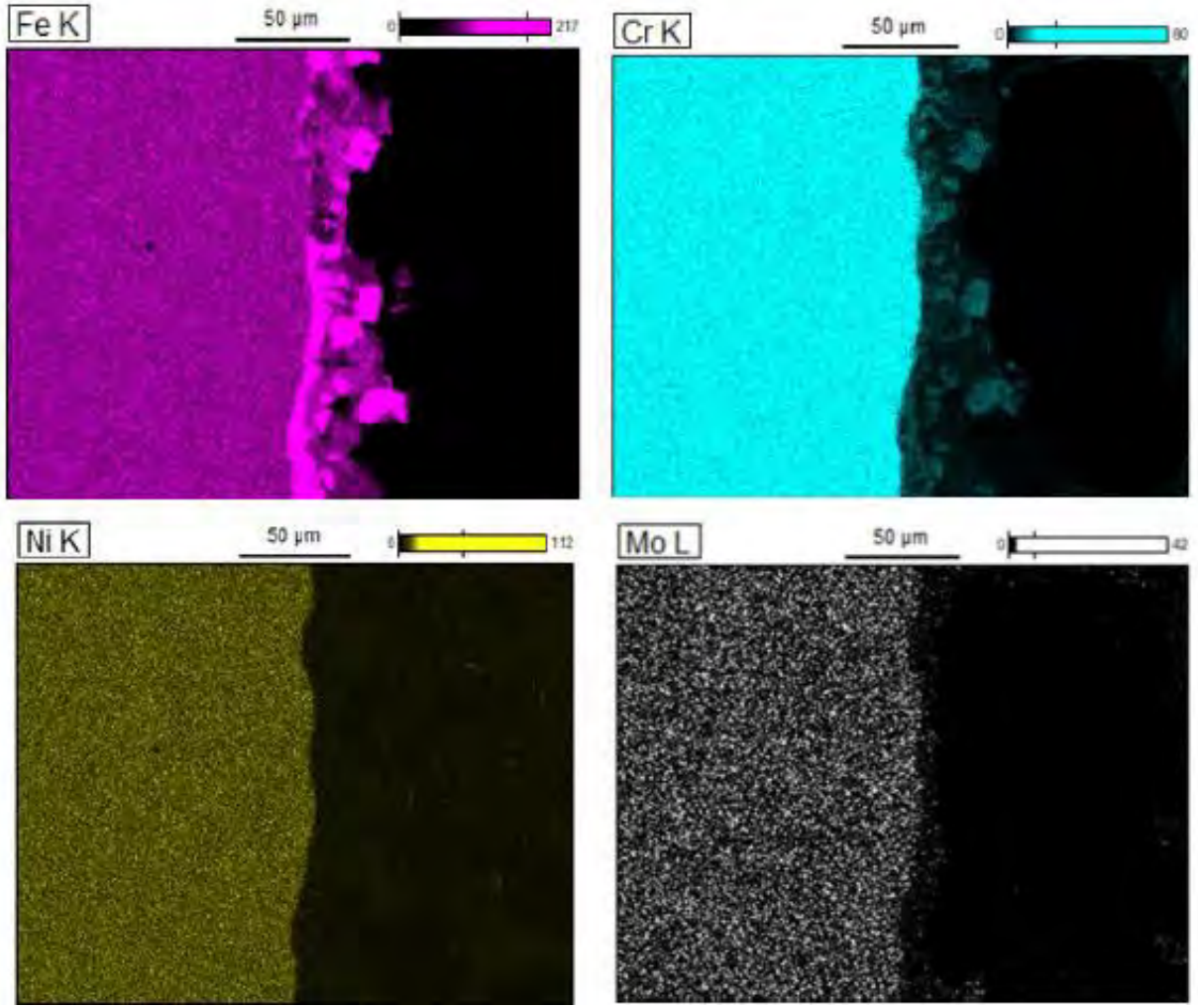

Typical Fe and Cr redeposition on the cold leg is observed

Modeling Mass Transport Using Radioisotope Tracers

- Rate equation for radioisotope N dissolving in the salt during the transit through the radioactive tube:

$$\frac{dN(t)}{dt} = -\lambda N(t) + S$$

S the coolant activation rate (atoms/cm3-sec)
Redeposition is not modeled (yet)

- Activity of radioisotope at the detection point (p) in the m recirculation cycle is:

$$\alpha_{m,p} = S\left(1 - e^{-\lambda t_1}\right)\frac{1 - e^{-m\lambda(t_1+t_2)}}{1 - e^{-\lambda(t_1+t_2)}}e^{-\lambda t_p}$$

t_1 time in contact with the irradiated tube
t_2 time in contact with non-irradiated metal,
t_p time to reach the point of detection in a given cycle

TRANSFORM Model (Scott Nelson, ORNL)

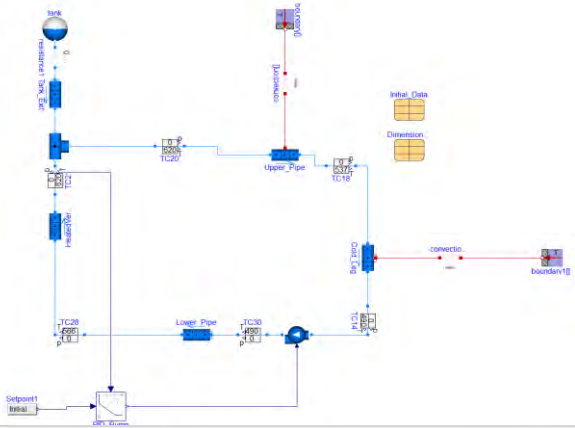

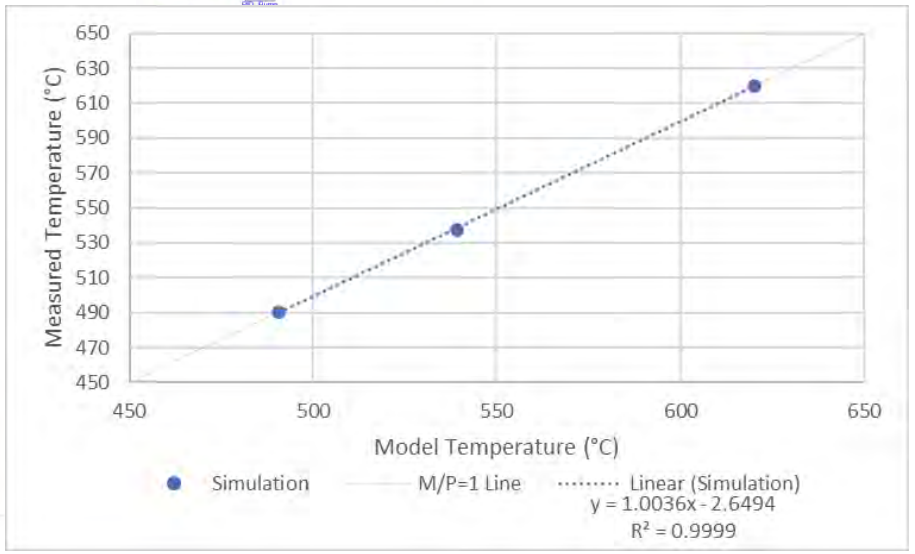

Output: Velocity ≈ 6.31 cm/s

Modeling Mass Transport Using Radioisotope Tracers

- Finding the source term **S**:
  - Using a second Fick's law type of diffusion modeling for radioisotope dissolution
  - Initial condition: $C_{\mathrm{Mn}^{52}}(x, 0)$ was determined (see earlier slides)
  - Boundary condition 1: $-\vec{J}_{\mathrm{Mn}^{52}}(x_{\mathrm{out}}, t) = 0$ - no flux at the outside surface of the tube
  - Boundary condition 2: $C_{\mathrm{Mn}^{52}}(0, t) = 0$
  - Use $D_{\mathrm{Mn}^{52}} = 10^{-17}\,\mathrm{m}^2/\mathrm{s}$ for Mn in 316L SS as reported in *"Smith, A. F. The tracer diffusion of transition metals in duplex oxide grown on a T316 stainless steel. Corros. Sci. 21, 517–529 (1981)".*

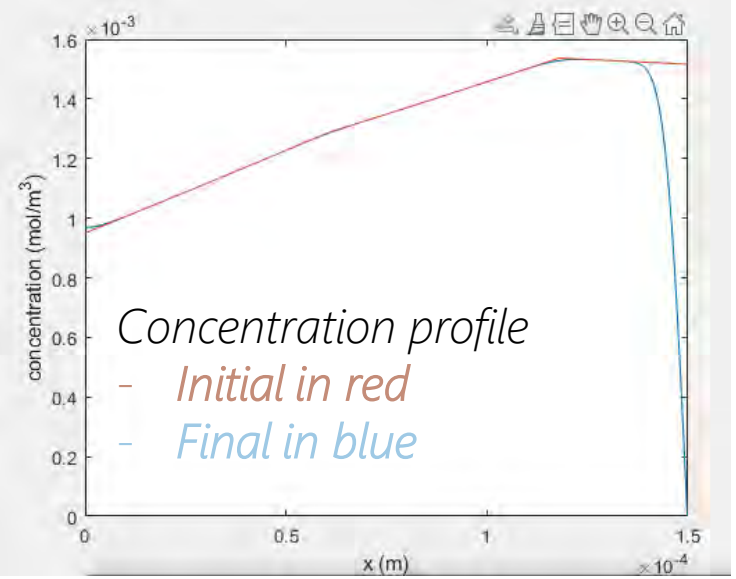

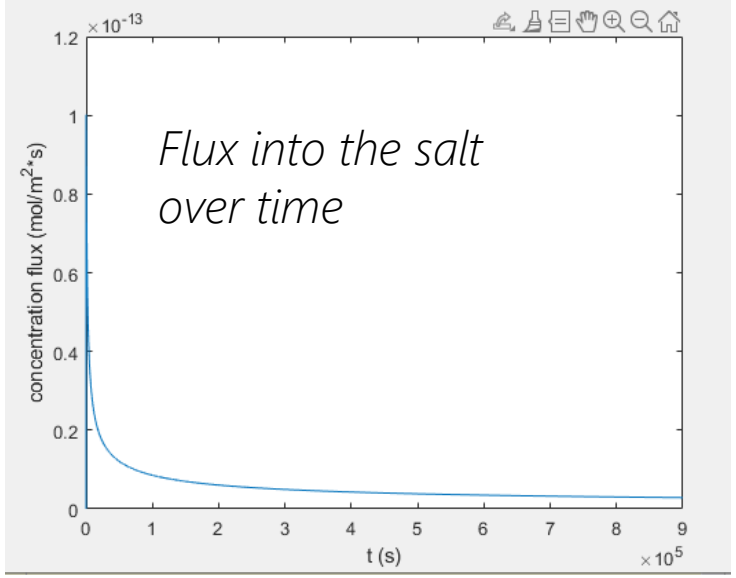

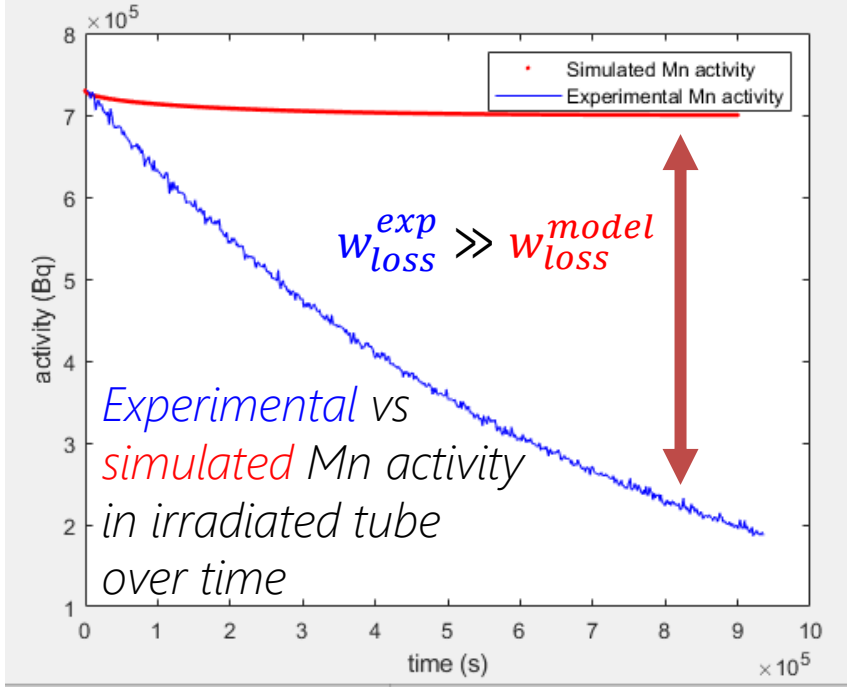

Modeling Mass Transport Using Radioisotope Tracers

- 1st hypothesis:

The reported diffusion coefficient of Mn in 316L SS is not accurate: $D_{\mathrm{Mn}^{52}} \neq 10^{-17}\mathrm{m}^2/\mathrm{s}$

→ We cannot fit the experimental data satisfactorily with an optimized diffusion coefficient!

- 2nd hypothesis:

$$C_{\mathrm{Mn}^{52}}(0,t) \neq 0$$

→ Likely but difficult to assess the right boundary condition…

- 3rd hypothesis:

The diffusion model is not physically correct

→ Let's implement constant surface recession rate in addition to Fick's diffusion → work in progress to obtain recession rate.

Modeling Mass Transport Using Radioisotope Tracers

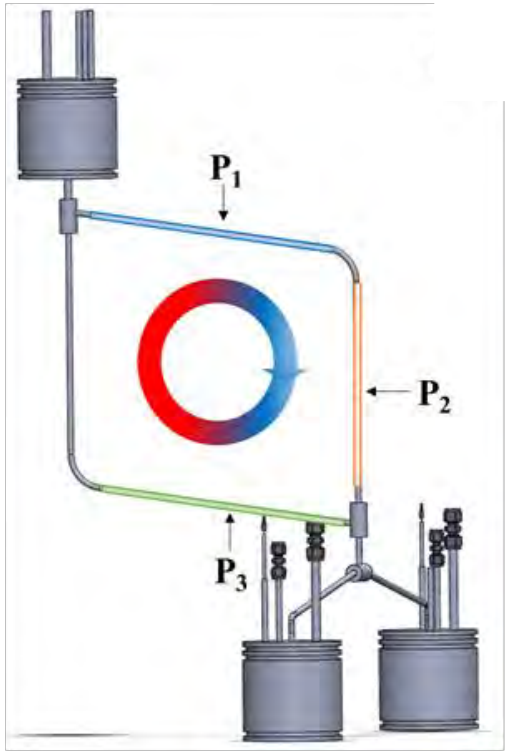

Measured activity at points 1, 2, and 3

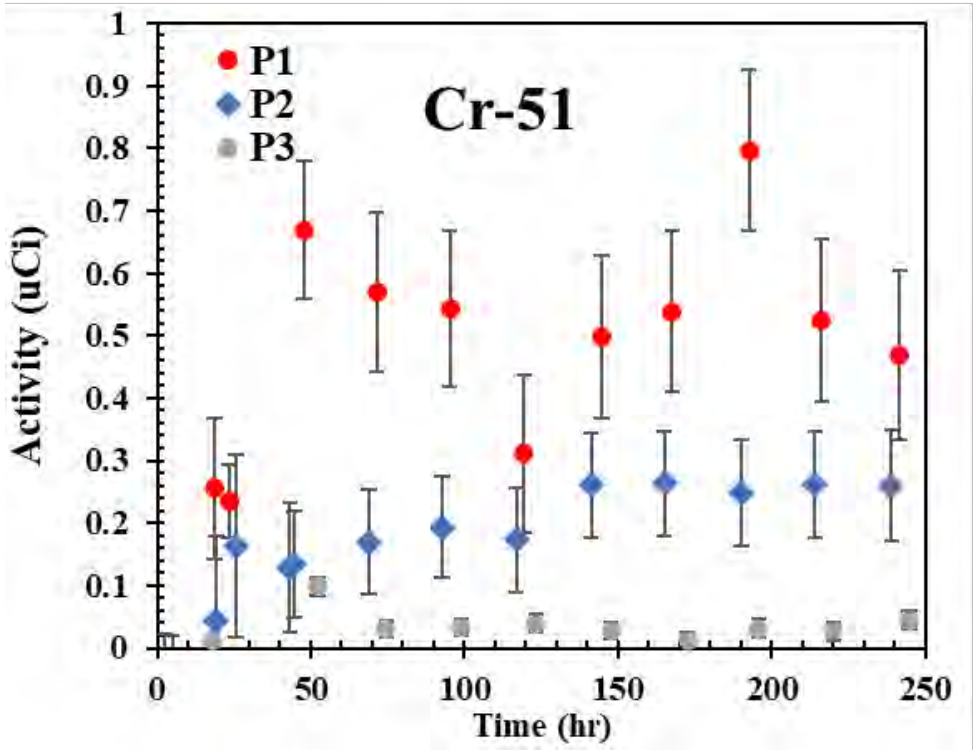

Activity level: $P_1 > P_2 > P_3$

- Next step is to include redeposition in the loop within the mass transport modeling and fit the model to the measured activities at different points → to be continued!
- We are moving forward with an Alloy 625 loop. Easy to source, of interest to industry. High Mo and high Cr, Mo for Tc radioisotope production and Cr for ^{51}Cr and ^{52}Mn production → ran for 2565 hours, still goiing

Alloy 625 Microloop: Cold Leg after 2565 hours

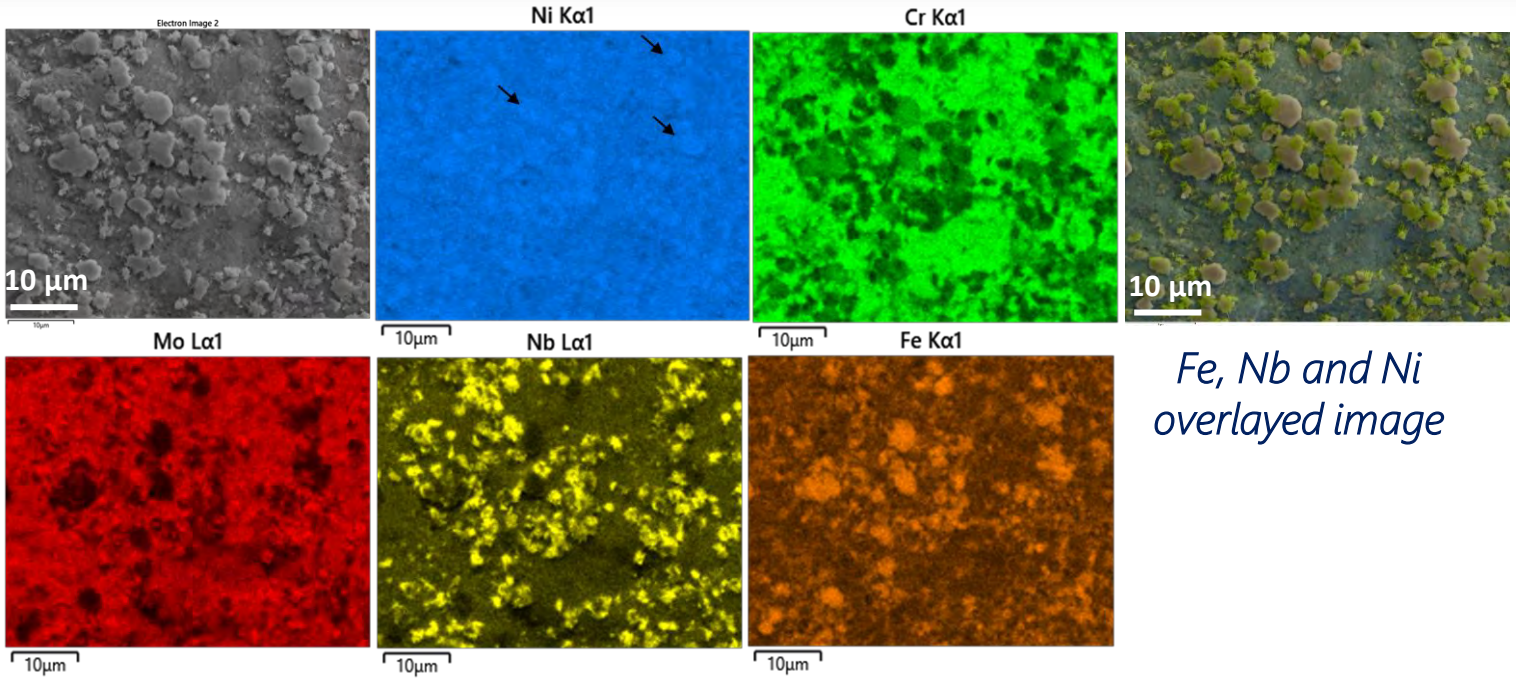

Fe, Nb and Ni overlayed image

Size distribution of Fe-deposits and δ–phase

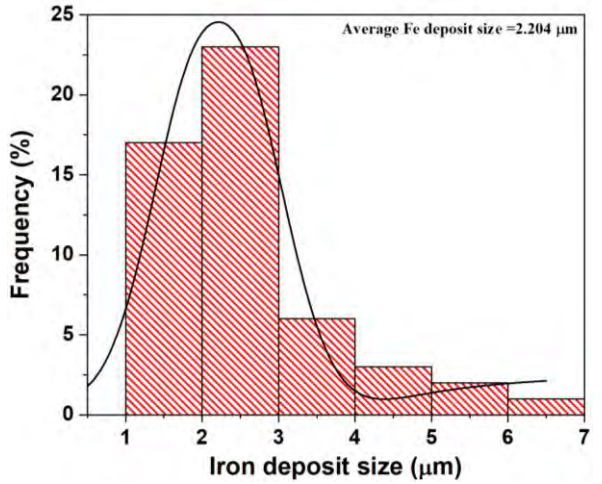

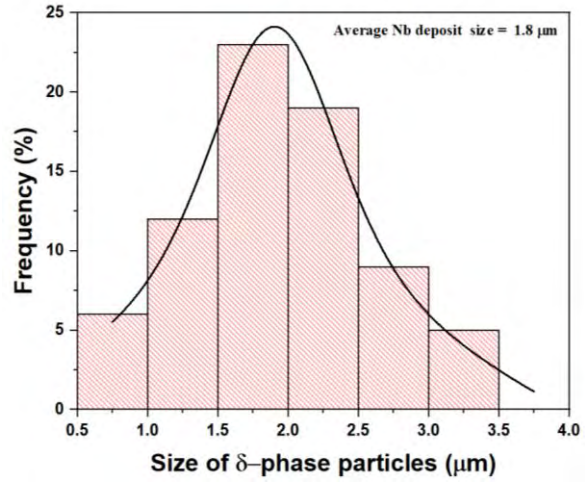

- The deposits are likely metallic. For Fe, the metal chloride is formed at the hot leg and transported in the salt along with the flow of molten salt.
- In EDS maps and point analysis (previous slide) showed wherever Nb precipitates are there, Ni and Mo also enriched indicating the formation of δ-Ni_3Nb/[Ni_3(Nb, Mo)].
- Both Fe deposits and the formed δ–phase have globular morphology with average size of 2.2 µm and 1.8 µm respectively.

Alloy 625 Microloop: Cold Leg after 2565 hours

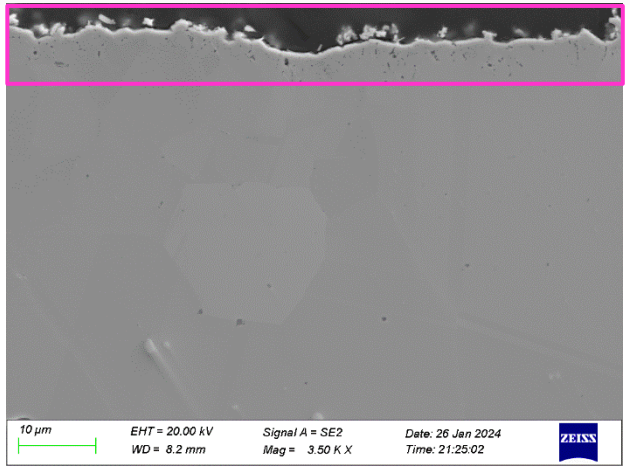

- No corrosion attack was observed at the cold leg salt/alloy interface.
- Deposits are formed at the interface.
- EDS maps showed enrichment of Ni, and Nb along Mo belonging to the **δ-** phase and also deposits of Fe.

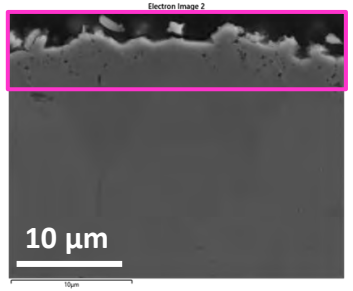

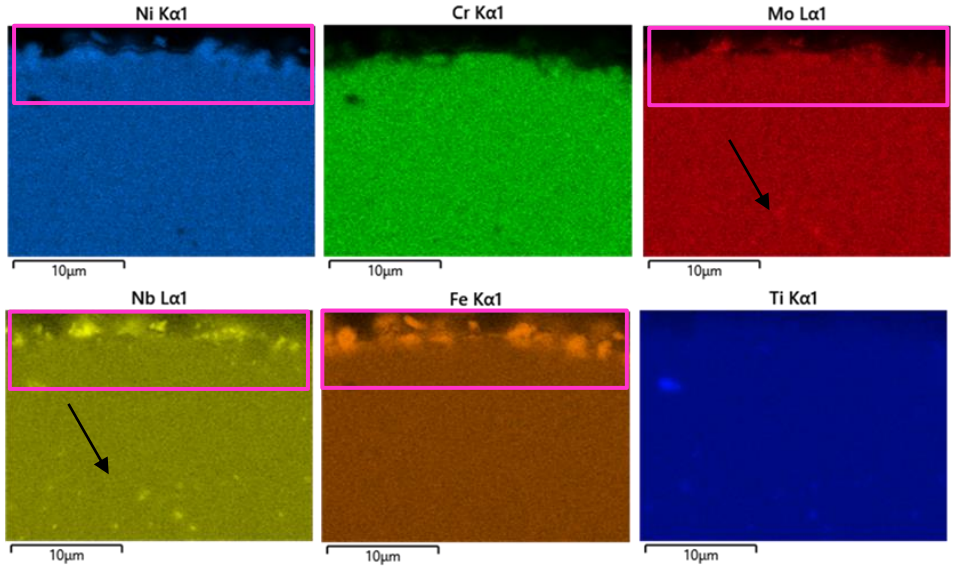

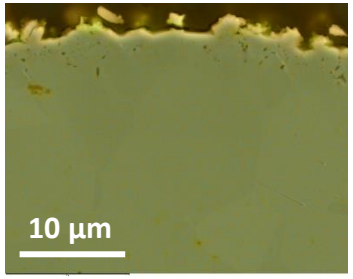

Fe, Nb and Ni overlayed image

Alloy 625 Microloop: Hot Leg after 2565 hours

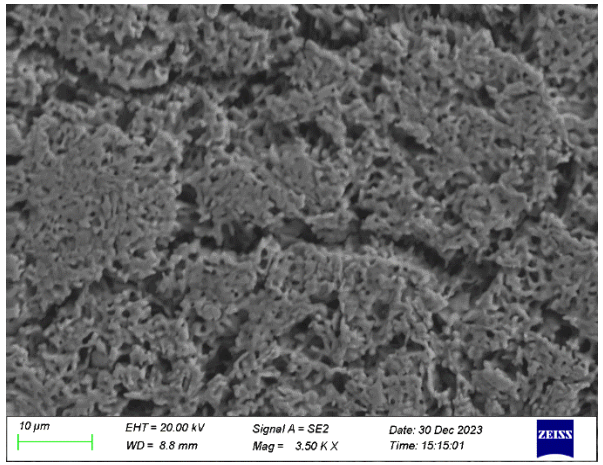

Element	Spectrum-1 (wt %)	Spectrum-2 (wt %)	Spectrum-3 (wt %)	Inconel-625 composition (wt %)
Ni	64.8	67.1	66.3	60.58
Cr	3.8	3.1	3.7	21.70
Mo	21.6	21.1	20.7	9.06
Nb	7.8	7.1	7.6	3.36
Fe	1.2	1.0	1.2	4.33
Ti	0.9	0.6	0.6	0.27

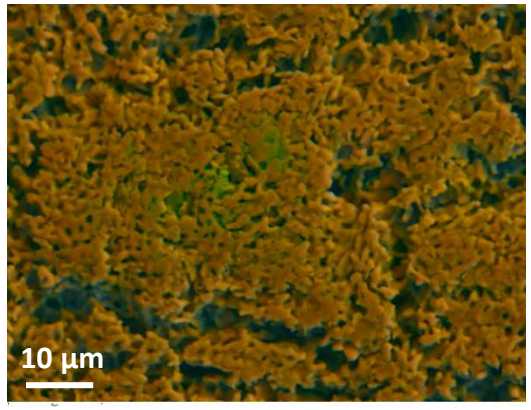

- Ligament morphology was observed.
- All spectra (1,2 and 3) show the enrichment of Ni, Mo and Nb and drastic depletion of Cr and Fe compared to the chemical composition of Inconel-625.
- Significant drop in Cr activity at the surface drives Mo to diffuse from bulk alloy to surface due to Mo activity gradient [8].

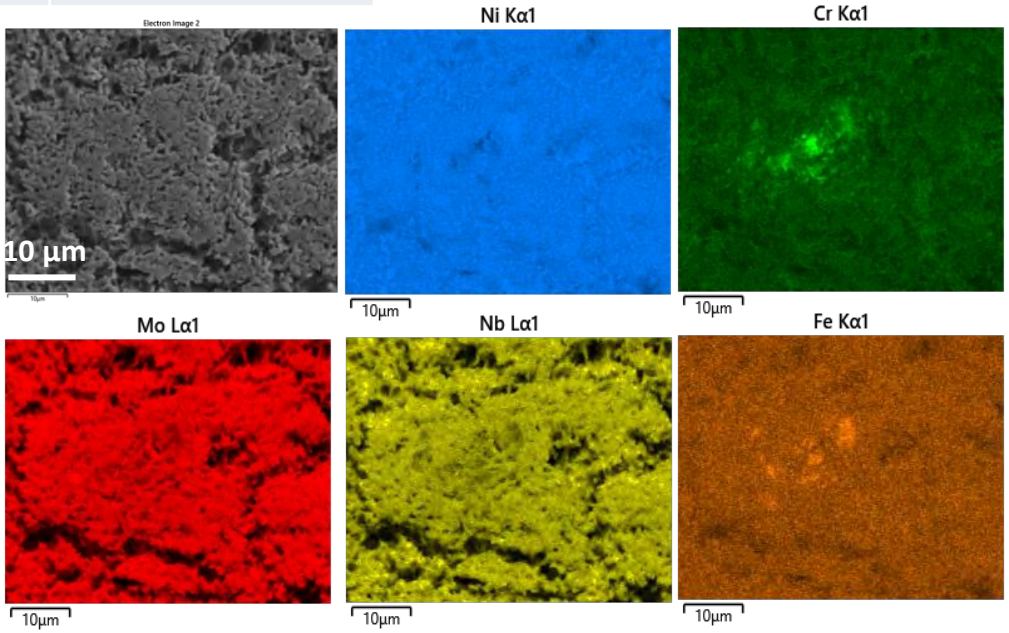

Alloy 625 Microloop: Hot Leg after 2565 hours

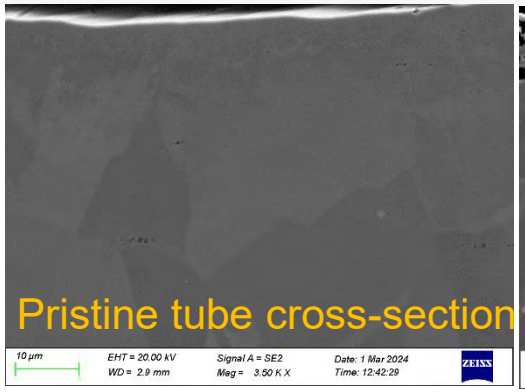

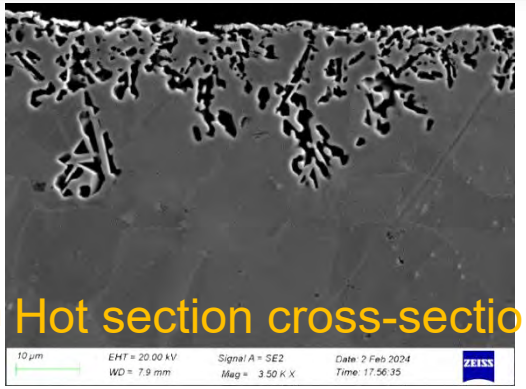

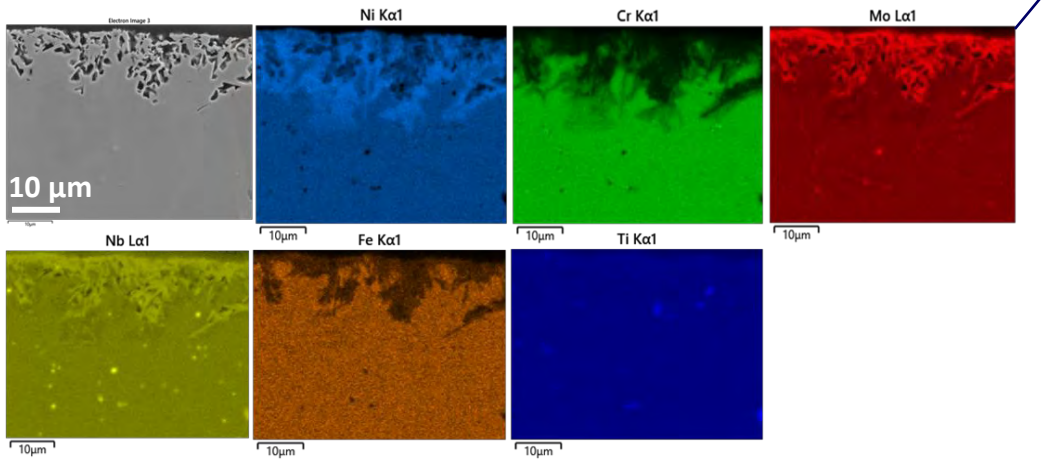

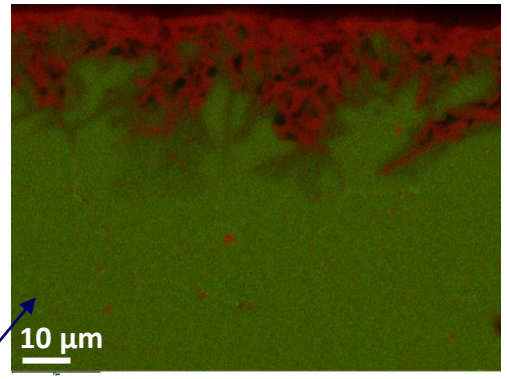

Cr and Mo overlayed image

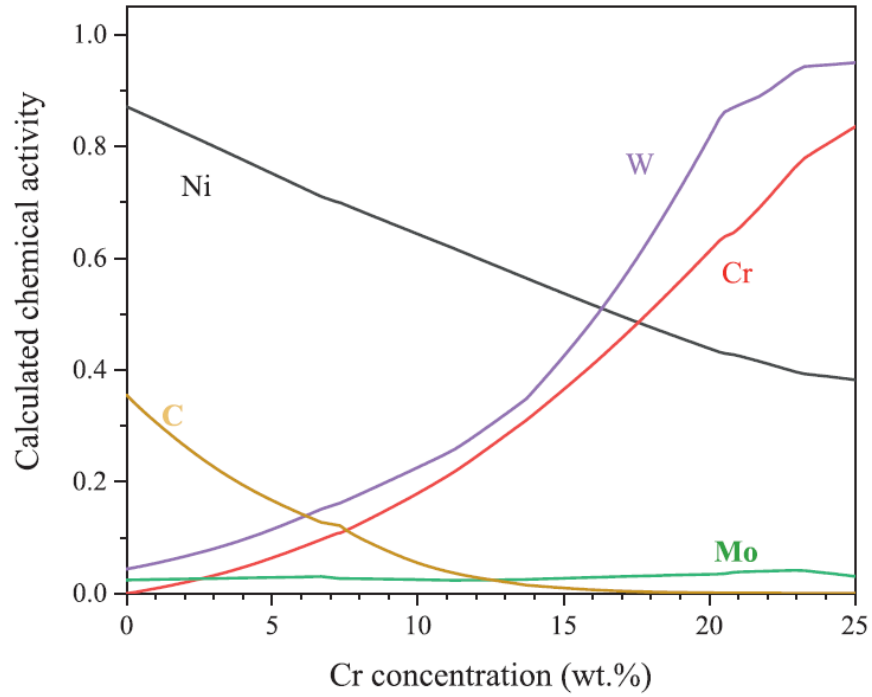

Calculated activities of different elements in alloy 230 as a function of Cr content.[8]

- Significant drop in Cr activity at the salt/alloy interface drives Mo to diffuse from bulk alloy to surface due to Mo activity gradient. This results in Mo enrichment at the surface. Cr dissolution can be decreased once the surface is enriched with Mo[8].
- A similar phenomenon can be expected for Nb.
- We are working with ORNL staff (Dr. Rishi) to model for a detailed understanding of this behavior for Inconel-625 alloy.

Alloy 625 Microloop: Results

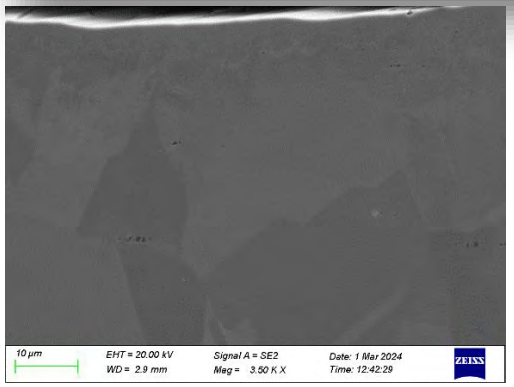

Pristine Inconel-625

Cold-section

497.6 ± 4.8°C

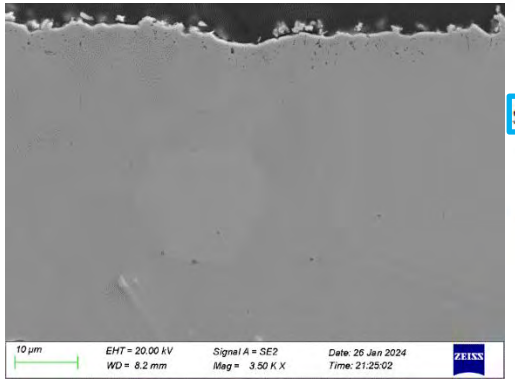

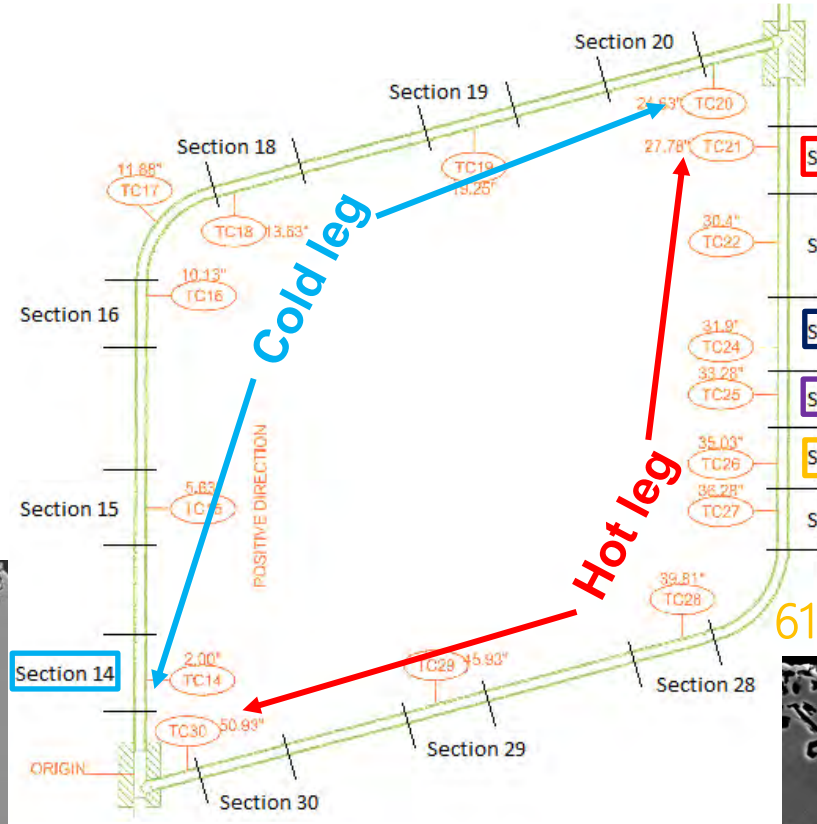

619.8 ± 0.2°C

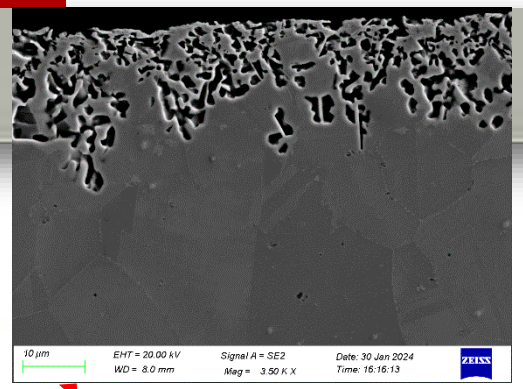

H-4

616.5 ± 0.5°C

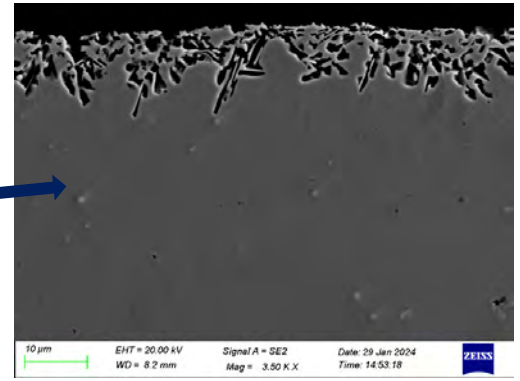

H-3

619.9 ± 0.4°C

H-2

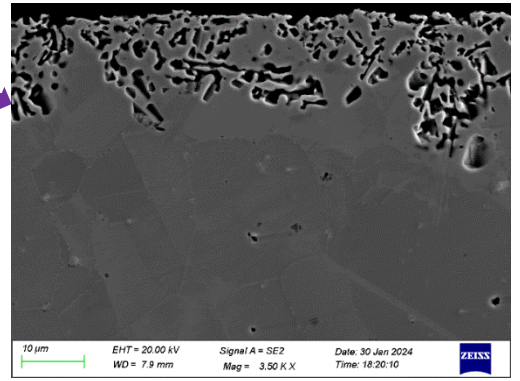

619.9 ± 0.2°C

H-1

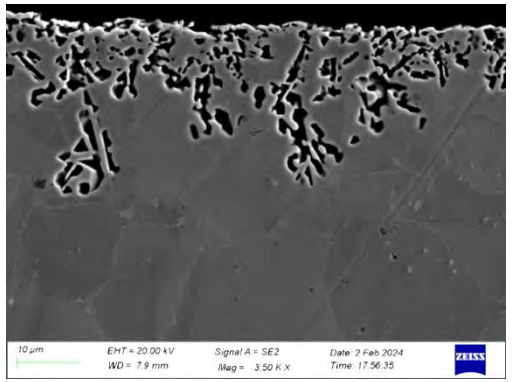

MADCOR

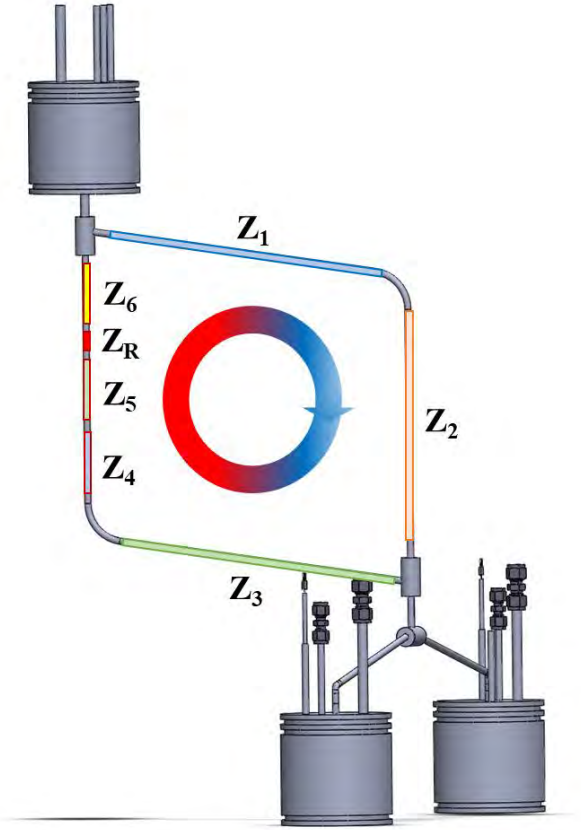

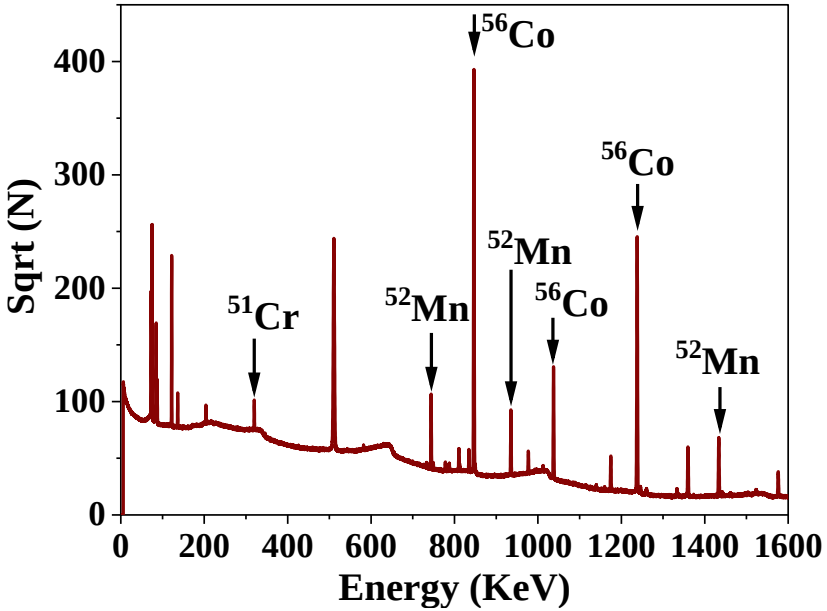

WISCONSIN
UNIVERSITY OF WISCONSIN–MADISON